HAIT Journal of Science and Engineering B, Volume 2, Issues 5-6, pp. 594-608

Randomized PWM for conductive EMI reduction in DC-DC choppers

Franc Mihalič* and Dejan Kos

Faculty of Electrical Engineering and Computer Science
University of Maribor, Smetanova 17, 2000 Maribor, Slovenia
**Corresponding author: fero@uni-mb.si*

Received 1 March 2005, accepted 10 June 2005

Abstract

In this paper, a comparative investigation of different random modulation schemes against the normal pulsewidth modulation (PWM) for the DC motor drive with step-down chopper (buck) and half-bridge configuration is presented. For this purpose, an experimental setup with DSP2 board has been developed. The board consists of the signal processor TMS320C32 which is suitable for verifying the different modulations strategies. The effectiveness of randomization on spreading the dominating frequencies that normally exist in constant-frequency PWM schemes is evaluated by the power spectral density (PSD) estimations in the low-frequency range. Finally, one universal demo board with two power converters configuration (driven by the micro controller PICF16F876) has been used in EMI measurements to comply with the CISPR 25 (or EN 55025) regulations.

1 Introduction

Recent electromagnetic interference (EMI) and electromagnetic compatibility (EMC) regulations such as FCC, VDE, CISPR, and EN have become tighter than ever [1, 2]. The modern power electronics is an engineering discipline that deals with the conversion of electrical power using fast semiconductor devices. These semiconductor devices are utilized as switches where the main designer's concern consists in reducing the power losses.

Switching operation generates signals with high du/dt and di/dt, and, consequently, wide bandwidths of disturbances. Because the power electronics equipment is usually connected to the supplying lines, those wide-band signals are travelling through them and pollute the electromagnetic environment with unwanted interference.

The EMC directive CISPR 25 emphasized an increasing awareness of EMC issues that highlight the conducted and radiated EMI problem of switching power converters in automotive environment [3]. Nowadays, human convenience in the cars enlarges the need for DC motor drive applications: electrical moving of mirrors, windows, water pump, etc. DC motors have variable characteristics and are used extensively in variable-speed drives. DC motors can provide a high starting torque and it is also possible to obtain speed control over a wide range. The methods of speed control are normally simpler and less expensive than those for AC drives. DC motor drives play also a significant role in modern industrial drives. With the recent advancements in power conversions, control techniques, and microcomputers, the AC motor drives are becoming increasingly competitive with DC motor drives. Although the future trend is toward AC drives, DC drives are currently used in many industries. It might be a few decades before the DC drives are completely replaced by AC drives.

2 Chopper drives

The chopper is used to control the armature voltage of a DC motor. The circuit arrangement of a chopper-fed DC motor is shown in Fig. 1a. Nowadays, the chopper switch is obviously a fast power MOSFET with very short switching times and low $R_{DC(on)}$ resistance what reduce the conductive losses but produce extremely high voltage- and current-rates (high EMI). It can be seen from Fig. 1a that output voltage of the chopper is always equal to the diode voltage drop $U_d \approx -0.6$ V. In order to increase the efficency of conversion, the synchronous buck configuration (half-bridge) has also been investigated (see Fig. 1b) where conductive losses of the MOSFET are lower than in the first case.

The average motor voltage is

$$U_M = U_D = DU_B \tag{1}$$

where D is the duty ratio of the chopper. In conventional DC-DC converters, the output voltage is generally controlled by varying the duty cycle of the main switch. The duty cycle and switching frequency are kept constant

in steady-state operation, so that the harmonic power of the input current and output voltage are concentrated at the multiples of the switching frequency. Using various random switching schemes, the harmonic power in the frequency domain can be spread, and the peak level of the power spectral density (PSD) becomes less than of the conventional PWM scheme. Discrete harmonics are significantly reduced, and the harmonic power is also spread over a continuous noise spectrum of small magnitude [4]. Spreading of harmonics energy across the spectrum may be carried out in various ways. Many randomization schemes and their syntheses have been addressed in many papers, dealing with: random switching control in DC-DC converters [5], acoustic noise reduction in sinusoidal PWM inverters [6], or improving the EMC of the boost rectifier [7].

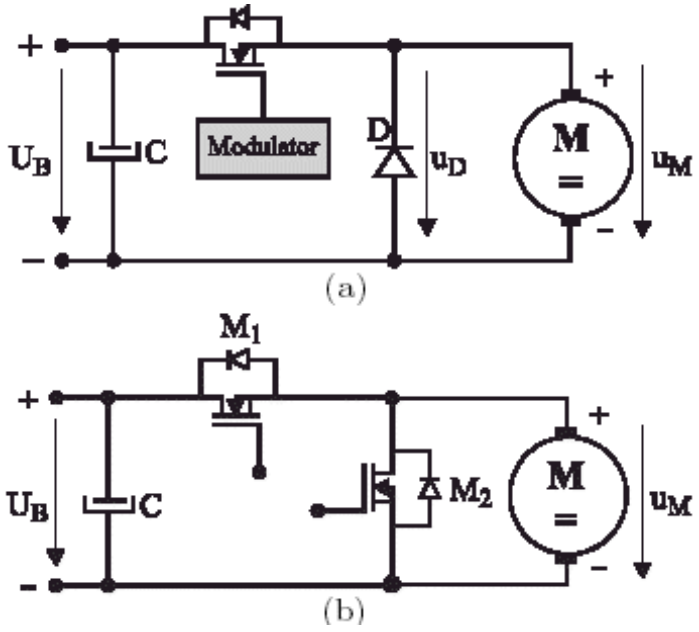

Figure 1: DC motor drives: (a) step-down chopper (buck), and (b) synchronous buck (half-bridge inverter).

In this paper, systematic investigation of the use of random modulation schemes in two types of DC-DC converters, namely the buck and synchronous buck converter, is present. The issues addressed include the effects of different randomized modulation strategies on the PSD and EMI optimizations and measurements in accordance with the CISPR 25 [3].

3 Random switching schemes

From several randomization modulation strategies, four of them are the most favoured: random pulse-position modulation (RPPM), random pulsewidth modulation (RPWM), and random carrier-frequency modulation with fixed duty cycle (RCFMFD) and with variable duty cycle (RCFMVD), respectively [8]. However, the suitability and effectiveness in the EMI reduction of each random modulation schemes in DC-DC converters have not been addressed, except in [7].

3.1 Characteristics of random modulation schemes

RPPM is similar to the classical PWM scheme with constant switching frequency. However, the position of the gate pulse is randomized within each switching period, instead of commencing at the start of each cycle. RPWM allows the pulsewidth to vary, but the average pulsewidth is equal to the required duty cycle. RCFMFD exhibits randomized switching period and constant duty cycle, while RCFMVD exhibits randomized switching period and constant pulsewidth. As the pulsewidth in RCFMVD is fixed and the switching period is randomized, the resultant duty cycle is also randomized. Nevertheless, the average duty cycle is equal to the desired value.

With the aid of Fig. 2, the pulse characteristics in each modulation scheme are summarized in Table 1.

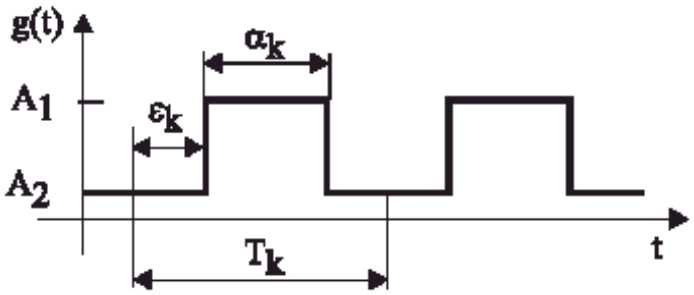

Figure 2: Switching signal in randomized modulation scheme.

The switching function $g(t)$ has two discrete levels (namely, A_1 and A_2), which are applicable to describe the behavior of classical DC-DC converters. T_k is the duration of the $k-$th cycle, α_k is the duration of the gate pulse

in $k-$th cycle, ε_k is the delay time of the gate pulse. The duty cycle of the switch d_k in the $k-$th cycle is equal to α_k/T_k.

Modulation	T_k	α_k	ε_k	$d_k = \alpha_k/T_k$
PWM	const.	const.	zero	const.
RPPM	const.	const.	rand.	const.
RPWM	const.	rand.	zero	rand.
RCFMFD	rand.	rand.	zero	const.
RCFMVD	rand.	const.	zero	rand.

Table 1: Characteristics of different random switching schemes.

3.2 Definition of the randomness level

In order to investigate the effectiveness of the stochastic variable randomness level on spreading harmonic power, a randomness level $\mathfrak{R}$ for each scheme is defined. For RPPM,

$$\mathfrak{R}_{RPPM}=\frac{\varepsilon_2-\varepsilon_1}{T_S} \tag{2}$$

where $\varepsilon_k \in [\varepsilon_1, \varepsilon_2]$, ε_1 and ε_2 are the minimum and maximum limits of the pulse position in each cycle with ε_1 obviously equal to zero, T_S is the nominal switching period.

For RPWM,

$$\mathfrak{R}_{RPWM}=\frac{\alpha_2-\alpha_1}{T_S}=d_2-d_1 \tag{3}$$

where $\alpha_k \in [\alpha_1, \alpha_2]$. Thus, the duty cycle d_k varies between the minimum possible value d_1 and the maximum possible value d_2 around the nominal duty cycle in classical PWM scheme.

For the RCFMFD and RCFMVD,

$$\mathfrak{R}_{RCFMFD}-\mathfrak{R}_{RCFMVD}=\frac{T_2-T_1}{T_S}. \tag{4}$$

In these two modulation schemes, T_k varies between the minimum possible T_1 and the maximum possible value T_2.

The duty cycle d_k in RCFMVD varies between $[(\alpha_k/T_2),(\alpha_k/T_1)]$, where α_k is fixed.

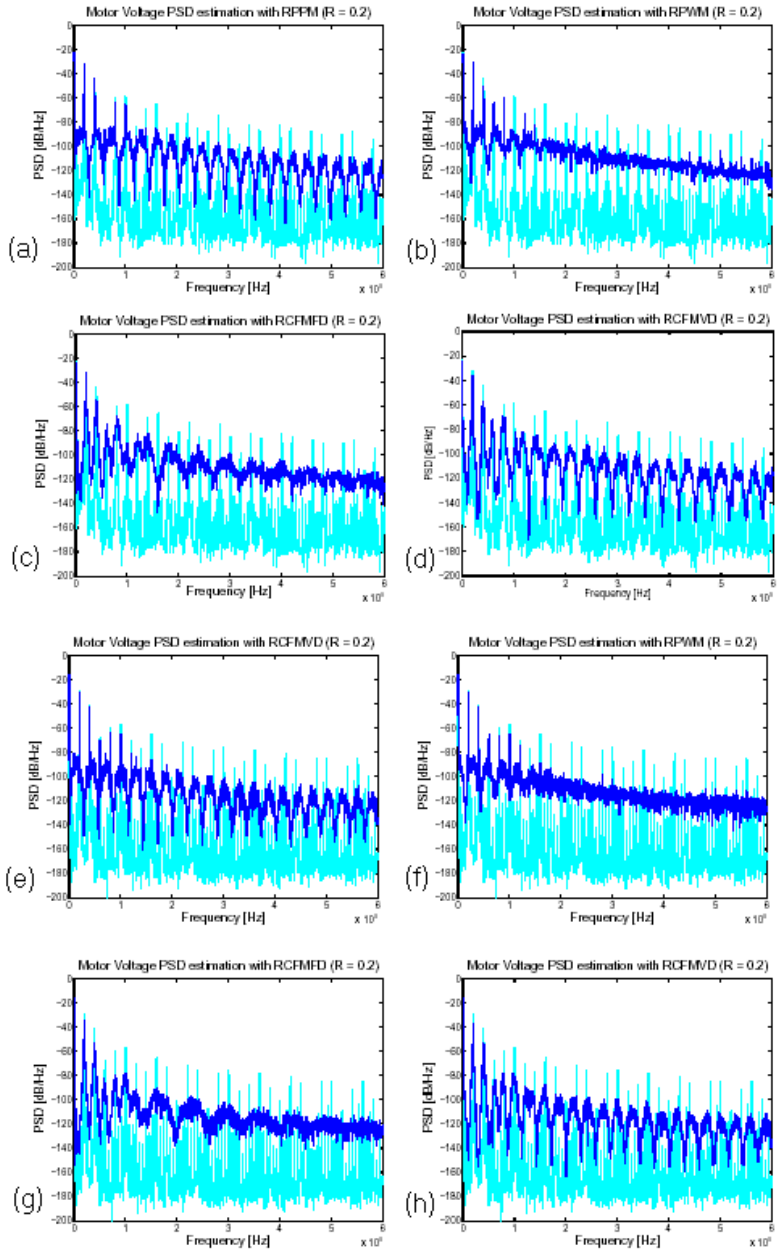

Figure 3: PSD estimations of the motor voltage at $\mathfrak{R}$ =0.2 in buck converter: (a) RPPM, (b) RPWM, (c) RCFMFD, (d) RCFMVD, and synchronous buck converter: (e) RPPM, (f) RPWM, (g) RCFMFD, (h) RCFMVD.

3.3 Power spectral density – PSD

We must note that harmonic spectrum in the case of randomized modulation scheme is random and each time different, therefore it must be evaluated by appropriate mathematical tools. Considering the random process theory, the natural quantity to study in a randomized switching setup is the power spectrum (the Fourier transform–FT of the autocorrelation function of a signal) and not the harmonic spectrum (i.e. the FT of the signal itself) [4,9]. In particular, the autocorrelation function of a random process is the appropriate statistical average that will be concerned with the characterizations of random signals in the time domain. The FT of the autocorrelation function gives the power spectrum density (PSD) and provides the transformation from the time domain to the frequency domain.

The PSD $S_p\left(f,\mathfrak{R}\right)$ of the transient waveform in Fig. 2 with RPPM and RPWM can be shown [4] to be equal to

$$S_p\left(f,\mathfrak{R}\right)=f_S\left\{E\left[\left|G(f)\right|^2\right]-\left|E\left[G(f)\right]\right|^2+f_S\left|E\left[G(f)\right]\right|^2\sum_{k=-\infty}^{\infty}\delta\left(f-kf_S\right)\right\} \tag{5}$$

where f_S is the nominal switching frequency, $G(f)$ is the FT of a cycle of switching function $g(f)$ with randomness level $\mathfrak{R}$, and $E[.]$ is the expectation operator taking over the whole ensemble. All PSD estimations have been done by using the Matlab software [10] and results are shown in Figs. 3a-d for the buck converter, and in Figs. 3e-f for the synchronous buck converter, respectively. All proposed and discussed randomized modulation strategies have smoothed power spectrums against the normal PWM where the switching power is dissipated in discrete multiples of the switching frequency. Most promising modulation schemes are the RPWM and RCFMFD shown in Figs. 3b, c, f, and g, respectively. Spreading the PSDs is a good prediction in reaching reduced conductive EMI at the input terminals, which is our main goal.

4 Electromagnetic interference – EMI

Exact prediction of EMI could help designer to satisfy EMI regulations cheaply and face with EMI problems easily before making the final hardware. Active components, such as switches and diodes, are the main noise sources in switched mode power supplies. Especially, the parasitic ringing voltage and current of the switches affect EMI pattern severely. However, not only an exact active component model is needed to predict accurate

ringing frequency, amplitude, overshoot, and rising/falling transient, but also electrical equivalent circuit of the printed circuit board (PCB) layout is necessary. Use of commercial simulation software, such a PSPICE [11], is sometimes difficult because of limited library models available. Recently, there is a huge amount of different Spice models available through the Internet, but inaccuracy of model parameter values for the purpose of good EMI simulations requires from the designer some expertise and practice.

4.1 Separately driven buck chopper and EMI

The hard switching buck chopper in Fig. 1 is a very basic converter, since the operation of many more complex converters can be derived from it. EMI noise generation involves both the typical converter operation and the parasitic stray components. According to their generation mechanisms, two different kinds of noise are distinguished: Common Mode (CM) noise and Differential Mode (DM) noise. DM noise is mainly caused by the pulsating converter current (see Fig. 4) and is attenuated by the input filter (Fig. 1). Since this capacitor is typically an electrolytic one with large ESL and ESR (in low temperature ELCO's), it is only effective for the reduction of DM noise up to the switching frequency.

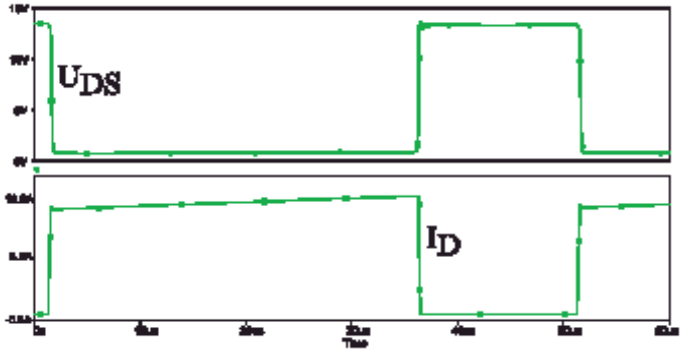

Figure 4: Sources of CM and DM noise.

CM noise is mainly due to high du/dt and high frequency oscillations produced by the interactions of the rapidly switching semiconductor devices (i.e. MOSFETs) with stray inductance. Contrary to DM noise, it occurs not between the two power lines of the converter but between the power lines and ground. When the converter interconnects are PCB tracks above

a groundplane, the CM current consists of a displacement current flowing through the parasitic track-to-groundplane capacitance.

In hard switching mode, contrary to soft switching mode, the switching device carries a full load current during turn-off, and sustains full voltage during turn-on (see Fig. 4). Since CM noise is strongly linked to voltage switching, and DM noise to current switching, CM and DM noise generations can take place simultaneously.

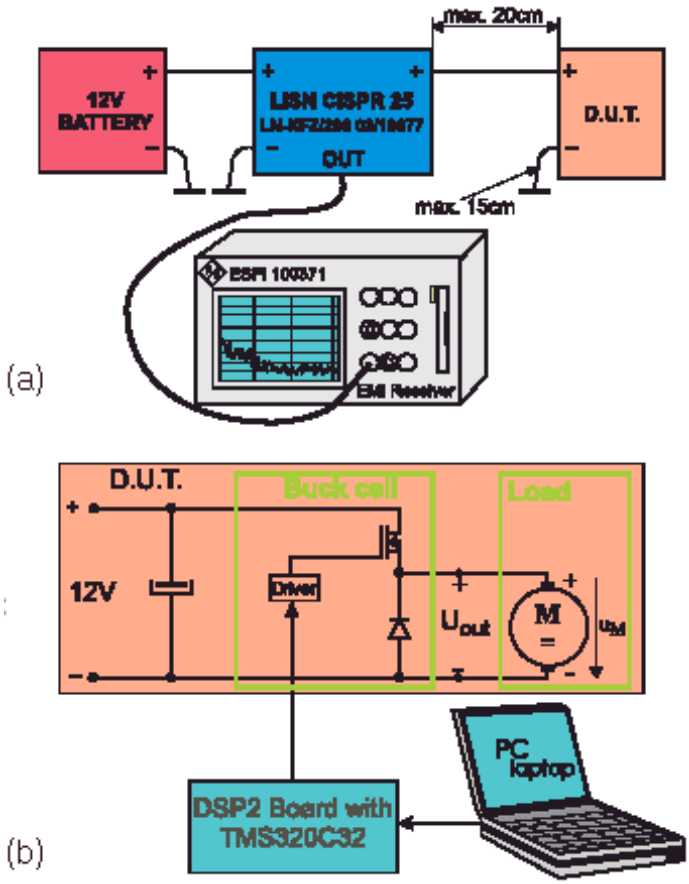

Figure 5: (a) Conductive EMI measurement setup for CISPR 25, and (b) device under test: buck chopper driven by the DSP2 board and personal computer.

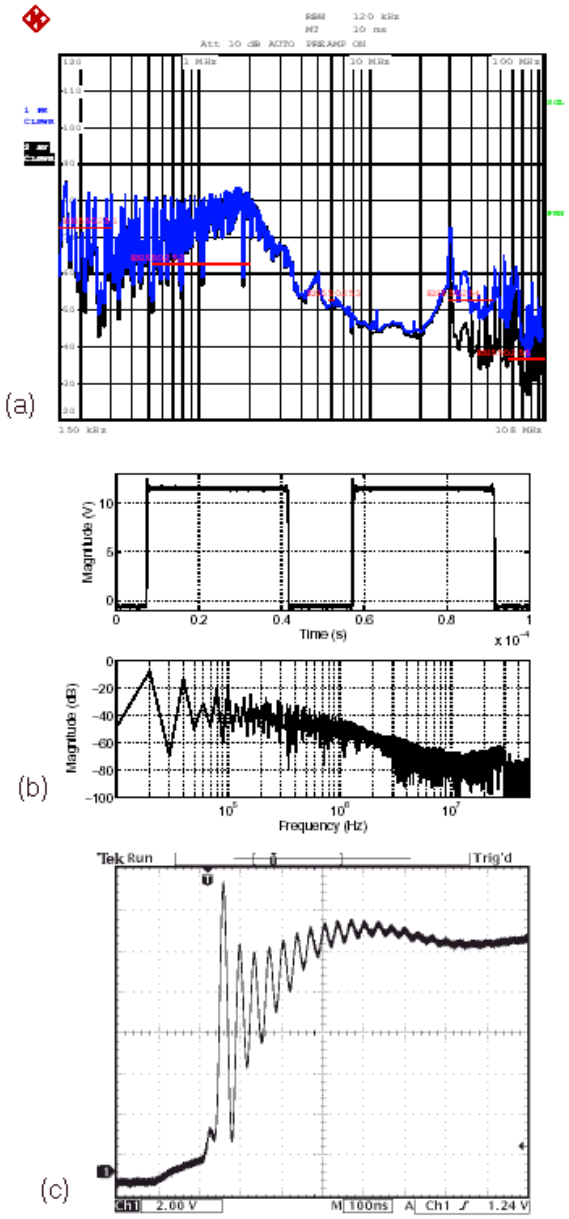

Figure 6: (a) Conductive EMI of PWM buck with DSP2 board and $D = 70\%$, (b) the output voltage and the harmonic spectrum, and (c) oscillations in the output voltage.

Completely equipped conductive noise measurement setup is shown in Fig. 5a, where the device under test (DUT) is one of the proposed buck choppers, and the line impedance stabilization network (LISN) is a stabilized low pass filtered network used to measure CM conducted emissions from power lines.

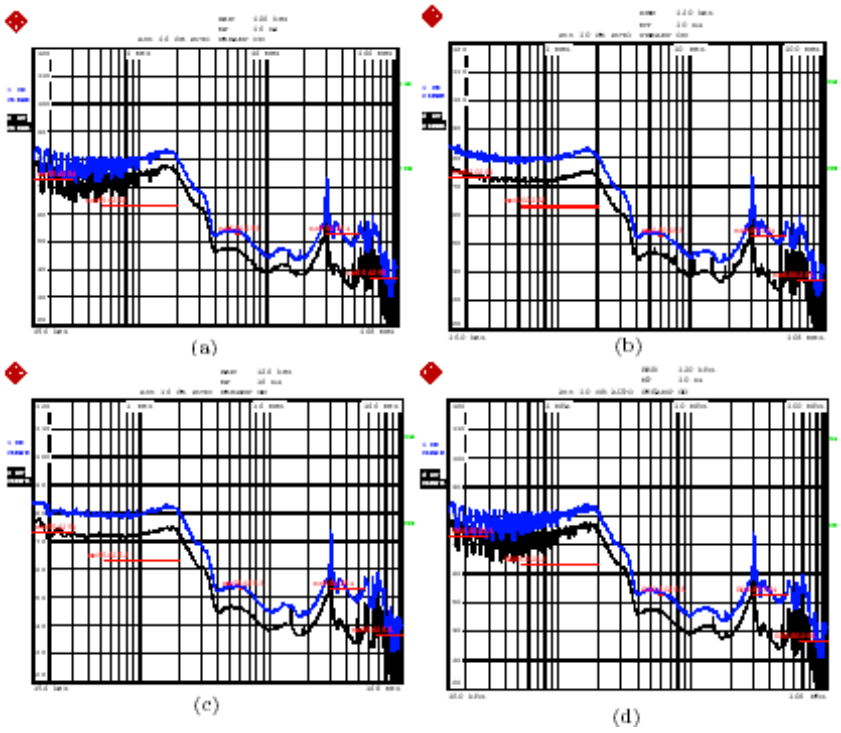

Figure 7: Conductive EMI of the randomized buck chopper with DSP2 board ($\mathfrak{R} = 20\%$, $D = 70\%$): (a) RPPM, (b) RPWM, (c) RCFMFD, and (d) RCFMVD.

The role of the LISN is to prevent noise from the power mains from contaminating the measurements, to present a relatively stable impedance to the product instead of the variable impedance of the power mains, and to fix the return path of the CM currents. In our case of testing, for compliance to conducted noise limits in CISPR 25, Class 5 [3], cables of significant length are inserted between the converter and LISN, as shown in Fig. 5a, respectively. DUT, driven by the DSP2 board with normal PWM and different randomized modulation schemes, is shown in Fig. 5b. As expected, such a

redundant buck converter setup (shown in Fig 1 and in Fig. 5b) results in a very high conductive noise measurements against the CISPR 25, shown in Fig. 6a. The reason for such a high level of conductive noise can be found in the hard switching of the main switch (as discussed before) and in the redundant power converter structure setup, which is constructed of the buck power cell, DSP2 signal processor board, and personal computer.

There is one very high peak in the conductive noise at 30 MHz in Fig. 6a, what can also be detected in the increased level of harmonic spectrum of the output voltage in Fig. 6b. The reason for additional noise above 50 MHz can be found in the very short rise-time and oscillations in the output voltage (see Fig. 6c).

Next, from the proposed randomized modulation schemes in Table 1 and based on PSD estimations results in Fig. 3, the RPPM has been performed and the result of EMI measurement is shown in Fig. 7a where the absolute (peak-to-peak) value of peak and average conductive noise is reduced in the whole freqency range. Even better is the result in case of RPWM (Fig. 7b), where the peak- and average value of conductive noise are smoothed, like in case of RCFMFD (Fig. 7c). The last randomized modulation scheme RCFMVD (in Fig. 7d) is very similar to the RPPM result.

The most promising fact is that in case of all randomized schemes the difference between the peak and the average value of the conductive noise is more or less than 8 dBμV, what is the very good starting point for improvements in the new circuit design (while in case of normal PWM the average and the peak value are always close to each other, see Fig. 6a).

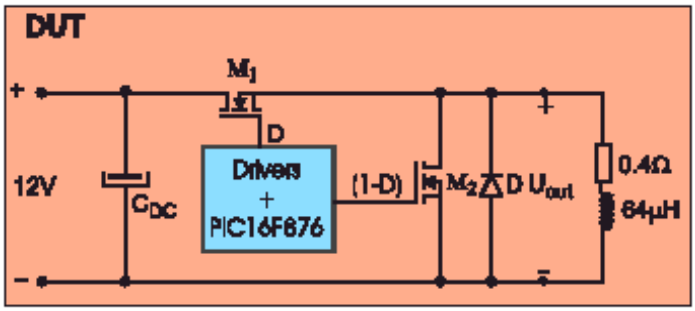

Figure 8: Improved DC-DC converter: synchronous buck.

Based on measured conductive noise in the evaluation system, we conclude to design a new demo board containing a buck power cell with driving

system (like μC PICF16F876), which can be uploaded with different modulation strategies. Finally, because of limited numerical capacity of the PIC micro controller, only one randomized modulation scheme has been implemented in the hardware, namely, the RPWM.

4.2 Synchronous buck chopper and EMI

As noticed before, the redundant working system of the power converter has resulted in exceedingly high conductive noise level against the CISPR 25. Therefore, new board for the DC-DC conversion with a self-running driving system has been constructed (quartz oscillator, μC PICF16F876 with PWM and RPWM, etc.), as shown in Fig. 8. The board is organized to work like

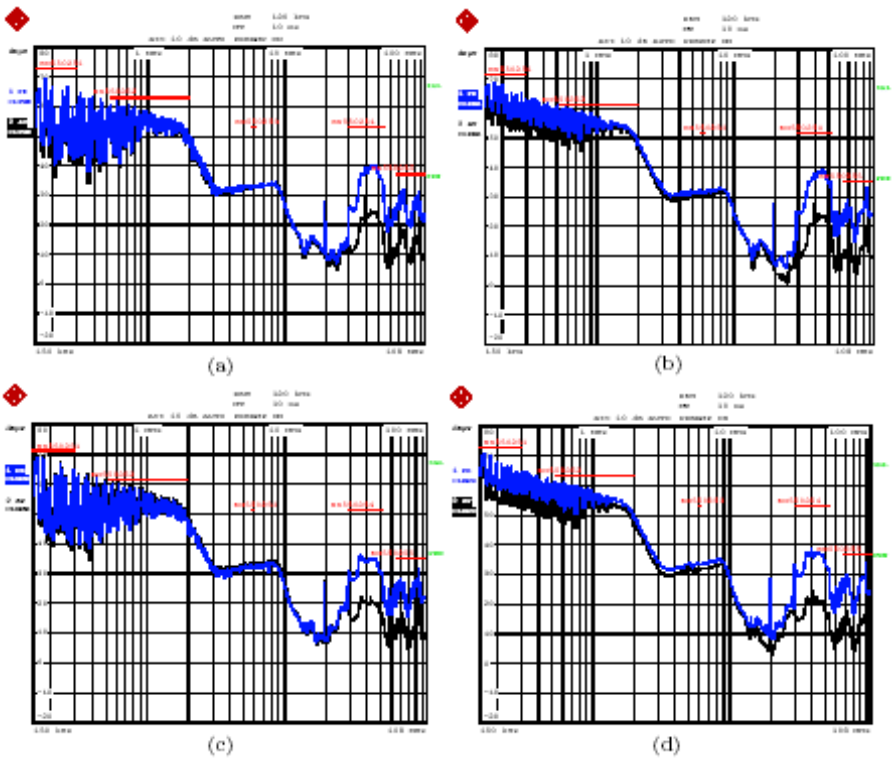

Figure 9: Conductive EMI of the improved buck chopper: (a) PWM ($D = 70\%$), (b) RPWM ($D = 70\%$, $\mathfrak{R} = 20\%$), and of the synchronous buck: (d) PWM ($D = 70\%$), (e) RPWM ($D = 70\%$, $\mathfrak{R} = 20\%$).

buck chopper or like synchronous buck converter (half-bridge), depending on driving two MOSFET switches. In the first case only M_1 is driven with the duty ratio D and M_2 is off, and in the second case both MOSFETs are switched simultaneously. For optimized high-frequency operation (low conducted EMI), several small ceramic capacitors near the DC-link capacitance are placed and to avoid the use of classic EMI filter at the input terminals for the low-frequency noise reduction, a modified turn-off snubber is connected to the high-side switch (R2CD-snubber), as reported in [12].

Since the setup components of the power converter are minimized (DSP2 board and PC were eliminated and PIC micro controller is uploaded with PWM or RPWM), the conductive EMI is evidently reduced (as shown in Fig. 9). While the snubber circuit is necessary in both converters (buck and synchronous buck), the randomized PWM effectively reduces conductive noise ripple in the low-frequency range up to 2 MHz (see Fig. 9b and 9d, respectively) and assures adequate difference between the peak- and average values of conductive noise.

5 Conclusion

This paper has given a comparative investigation of four different random modulation schemes on the PSD and conductive EMI. It has been clearly demonstrated that all considered randomization schemes can gradually spread the discrete frequency harmonic power over the whole frequency spectrum. However, this investigation shows that among all random schemes under consideration, the RPWM and RCFMFD give the minimum low-frequency harmonic spectrum and, therefore, can be considered as the best choice for DC-DC converter application. Nevertheless, because of PIC16F876 micro controller arithmetic limitations, only the RPWM has been implemented and verified in EMI measurements.

References

[1] J.J. Goedbloed, *Electromagnetic Compatibility* (Prentice Hall, NY, 1992).

[2] R. Redl, IEEE Power Electronics Specialists Conference, PESC'96, p.15 (1996).

[3] EN 55025 Document, *Radio disturbance characteristics for protection of receivers used on board vehicles, boats, and on devices – Limits and methods of measurements* (2004).

[4] A.M. Stanković, G.C. Verghese, and D.J. Perreault, IEEE Trans. on Power Electronics **10**, 680 (1995).

[5] T. Tanaka, T. Ninomiya, and K. Harada, IEEE Power Electronics Specialists Conference, PESC'89, p.500 (1989).

[6] T.G. Habetler and D.M. Divan, IEEE Trans. on Power Electronics **6**, 356 (1991).

[7] F. Mihalič, M. Milanovič, and C. Couto, International Journal of Electronics **90**, 235 (2003).

[8] K.K. Tse, H.S. Chung, S.Y.R. Hui, and H.C. So, IEEE Trans. on Industrial Electronics **47**, 253 (2000).

[9] S.L. Marple. *Digital Spectral Analysis with Applications* (Prentice Hall, Engelwood Cliffs, NJ, 1987).

[10] Matlab: *Signal Processing Toolbox User's Guide* (The MathWorks, Nattick, MA, 1994).

[11] PSpice A/D, OrCAD, Cadence Design Systems Inc., CA. Available: http://www.orcad.com/products/pspice/.

[12] D. Kos, F. Mihalič, and K. Jezernik, IEEE International Symposium on Industrial Electronics, ISIE'05, p.441 (2005).